Applied Thermal Engineering ■■ (2016) ■■–■■

Contents lists available at ScienceDirect

Applied Thermal Engineering

journal homepage: www.elsevier.com/locate/apthermeng

Research Paper

Exergy-based operation optimization of a distributed energy system through the energy-supply chain

Bing Yan [a], Marialaura Di Somma [b,c,*], Nicola Bianco [b], Peter B. Luh [a], Giorgio Graditi [c], Luigi Mongibello [c], Vincenzo Naso [b]

[a] Department of Electrical and Computer Engineering, University of Connecticut, Storrs, CT 06269, USA
[b] Dipartimento di Ingegneria Industriale (DII), Università degli Studi Federico II, Napoli 80125, Italy
[c] ENEA – Italian National Agency for New Technologies, Energy and Sustainable Economic Development, CR Portici, Portici 80055, Italy

HIGHLIGHTS

- Exergy-based operation optimization of a Distributed Energy System.
- Exergy losses modeled for the energy devices at the energy conversion step.
- Multi-objective optimization problem to reduce energy costs and exergy losses.
- Problem solved by surrogate Lagrangian relaxation combined with branch-and-cut.
- Reduced waste of high-quality energy resources by reduction of exergy losses.

ARTICLE INFO

Article history:
Received 1 September 2015
Accepted 7 February 2016
Available online

Keywords:
Exergy losses
Distributed energy system
Surrogate lagrangian relaxation

ABSTRACT

Developing sustainable energy systems is crucial in today's world because of the depletion of fossil energy resources and global warming problems. Application of exergy principles in the context of energy supply systems may achieve efficient energy-supply chains and rational use of energy in buildings. This paper presents an exergy-based operation optimization of a distributed energy system by considering the whole energy-supply chain from energy resources to user demands. The problem is challenging in view of the complicated interactions of energy devices and the modeling of exergy losses. To capture these complicated interactions, energy networks are established with exergy losses modeled at the energy conversion step, which accounts for the largest part of the total exergy loss in the whole energy-supply chain. A multi-objective mixed integer programming problem is formulated. The problem is efficiently solved by the novel integration of surrogate Lagrangian relaxation and branch-and-cut. The Pareto frontier, including the best possible trade-offs between the economic and exergetic objectives, is obtained by minimizing a weighted sum of the total energy cost and total exergy loss occurring at the energy conversion step. Results demonstrate that the use of high-quality energy resources is reduced by the reduction of exergy losses, leading to sustainability of energy supply systems.

1. Introduction

Developing sustainable energy systems is becoming more and more important in today's world because of the depletion of fossil energy resources and the related global warming problems. Therefore, high-quality energy carriers, such as fossil fuels and electricity, should be efficiently used [1]. Buildings are responsible for more than 40% of the total final energy consumption on a worldwide scale [2]. A significant share of this energy consumption is for space heating (SH) and cooling, and domestic hot water (DHW) demands. These are low-quality energy demands because of the associated temperatures required. However, thermal demands in buildings are commonly met by high-quality energy resources. There is great potential in energy-management of energy supply systems to attain efficient energy-supply chains and rational use of energy in buildings [3].

Current analyses and optimization methods for energy-management of energy supply systems do not distinguish different qualities of energy flows. In thermodynamics, the quality of an energy carrier is measured by exergy. Exergy is defined as the maximum theoretical work that can be obtained from an energy flow, as it comes to the equilibrium with the reference environment [1,3–7]. The concept of exergy was introduced in building

* Corresponding author. Tel.: +39 0817723204; +39 3492963733.
E-mail addresses: marialaura.disomma@unina.it; marialaura.disomma@enea.it (M. Di Somma).

http://dx.doi.org/10.1016/j.applthermaleng.2016.02.029
1359-4311/

efficiency studies by international research projects, such as ECBCS Annex 37 [5], and Annex 49 [1]. Several studies on the exergy analysis of energy supply systems for the building environment are also found in recent years [6,8–10].

A distributed energy system (DES) is an energy system where energy is made available close to energy end-users [11]. DESs provide a unique opportunity to show the benefits of the exergy analysis for preserving high-quality energy resources, since several energy devices convert a set of primary energy carriers (e.g., electricity, solar energy, natural gas) with different energy quality levels to satisfy end-user demands with different energy quality levels. In terms of DESs, most of the studies in the literature are focused on the operation optimization of DESs to reduce energy costs [12–14], which is essential in the short run. The optimized operation strategies of a DES were obtained in a previous work [15] to reduce the total daily energy cost and increase the total exergy efficiency. For simplicity, the total exergy input to the DES and the total exergy output required to meet the energy demands were considered instead of the exergy input and output of each energy device in the energy-supply chain.

This paper presents an exergy-based operation optimization of a DES through the energy-supply chain from energy resources to user demands (electricity, SH and DHW demands are considered), without neglecting the energy costs. The main goal is to obtain the optimized operation strategies of the DES to reduce the total energy costs and the total exergy loss occurring at the energy conversion step, which accounts for the largest part of the total exergy loss in the whole energy-supply chain. By reducing these exergy losses, the use of high-quality energy resources can be reduced, leading to sustainability of energy supply systems.

The optimization problem is challenging since several energy devices convert a set of input energy carriers, such as natural gas, electricity, and solar energy, into output energy carriers, such as heat and electricity, with complicated interactions among them; the exergy of thermal energy is directly related to the temperature and the mass flow rate of the corresponding energy carrier, and the problem is nonlinear. To capture the complicated interactions, energy networks are established from energy resources to user demands, based on the physical structure of the energy-supply chain. Exergy losses are then modeled for the energy devices at the conversion step based on the networks to make visible where and how much exergy is lost. A multi-objective mixed-integer problem is formulated. The objective is to minimize a weighted sum of the total energy cost and exergy losses at the energy conversion step while satisfying given time-varying user demands. Surrogate Lagrangian relaxation and branch-and-cut are integrated in a novel way for a speedy and near-optimal performance. The Pareto frontier, consisting of the best possible trade-offs between the economic and exergetic objectives, is obtained. Results show that the use of high-quality energy resources can be reduced by the reduction of exergy losses, leading to sustainability of energy supply systems.

2. Problem formulation

To match the solution methodology, the surrogate Lagrangian relaxation combined with branch-and-cut method, a separable and linear formulation, is preferred to solve the problem efficiently. The energy-supply chain under consideration consists of energy conversion devices, including gas turbine and heat recovery boilers, as the combined heat and power (CHP) system, solar thermal plant, auxiliary natural gas boilers, and heat pump; thermal energy storages, distribution devices (e.g., water pipes) as well as terminal devices (e.g., fan coils for SH) are also considered as shown in Fig. 1. Electricity is 100% exergy (fully convertible into useful work), while the exergy of thermal energy is directly related to the temperature and mass flow rate of the corresponding energy carrier. The energy networks for space heating and domestic hot water demands need to be established based on the physical structures of water pipes, valves, mixers, etc.

The general structure of the energy and exergy modeling and common constraints of energy devices are first described as follows.

Capacity constraints. The energy generation rate (e.g., electricity and heat) of the device, $R_{ED}(t)$, should be within its minimum and maximum values if it is on (xED (t) = 1):

$$x_{ED}(t)R_{ED}^{\min} \le R_{ED}(t) \le x_{ED}(t)R_{ED}^{\max} \tag{1}$$

Ramp rate constraints. The variations in energy generation rates between two successive time intervals should be within the ramp-down, DRED, and ramp-up, URED:

$$-DR_{ED} \le R_{ED}(t) - R_{ED}(t-\Delta t) \le UR_{ED} \tag{2}$$

where Δt is the length of the time interval.

Energy consumption. The input rate of the energy source, $S_{ED}^{in}(t)$, required by the energy device to provide the output energy rate, $R_{ED}(t)$, is:

$$S_{ED}^{inp}(t) = R_{ED}(t)/\eta_{ED} \tag{3}$$

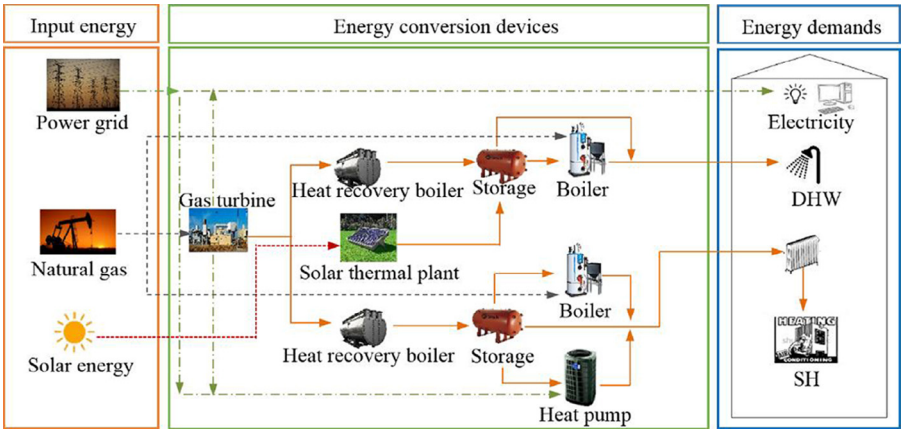

Fig. 1. Scheme of the energy-supply chain.

Please cite this article in press as: Bing Yan, et al., Exergy-based operation optimization of a distributed energy system through the energy-supply chain, Applied Thermal Engineering (2016), doi: 10.1016/j.applthermaleng.2016.02.029

where η_{ED} is the conversion efficiency of the device.

Exergy loss. The input exergy rate and output exergy rate of the device depend on the type of the energy carrier, and the exergy loss rate is formulated as the difference of them.

Modeling of the electricity network, energy networks for space heating, and for domestic hot water is presented in Subsections 2.1, 2.2, and 2.3, respectively. Objective functions and multi-objective optimization method are discussed in Subsection 2.4.

2.1. Modeling of electricity network

Since electricity is 100% exergy, the exergetic modeling of the electricity network is mainly the energy modeling.

2.1.1. Modeling of the gas turbine in the CHP system

The CHP system may consist of multiple gas turbines for electricity and the corresponding heat recovery boilers, using high-temperature exhaust gas to satisfy demands of space heating and domestic hot water [16]. For simplicity, one gas turbine is considered here. The modeling of multiple gas turbines is similar, and the problem complexity may increase as the number of gas turbines increases. Constraints considered for the gas turbine are presented below.

The volumetric flow rate of natural gas, $\dot{G}_{GT}(t)$, required by the gas turbine to provide the electricity rate, $\dot{E}_{GT}(t)$, is:

$$\dot{G}_{GT}(t) = \dot{E}_{GT}(t)/(\eta_e LHV_{NG}) \tag{4}$$

where η_e is the turbine gas-to-electric efficiency and LHV_{NG} is the lower heat value of natural gas.

The heat rate of the exhaust gas recovered from the gas turbine, $\dot{Q}_{GT}^{exgas}(t)$, is:

$$\dot{Q}_{GT}^{exgas}(t) = \dot{E}_{GT}(t)(1-\eta_e-\mu_{GT})/\eta_e \tag{5}$$

where μ_{GT} is the fraction of heat lost in the gas turbine.

For the gas turbine, the input energy carrier is natural gas. The specific chemical exergy of natural gas is the maximum work that can be obtained from the substance, by taking it to the chemical equilibrium with the reference environment at the constant temperature and pressure [17]. The exergy input rate of natural gas to the gas turbine, $\dot{E}x_{GT}^{NG}(t)$, is the gas volumetric flow rate consumed, $\dot{G}_{GT}(t)$, multiplied by the specific chemical exergy of natural gas, ex_{NG}:

$$\dot{E}x_{GT}^{NG}(t) = ex_{NG}\dot{G}_{GT}(t) \tag{6}$$

The specific chemical exergy of natural gas, ex_{NG}, can be evaluated by multiplying the exergy factor, ς_{NG}, and the lower heat value, LHV_{gas}:

$$ex_{NG} = \varsigma_{NG} LHV_{NG} \tag{7}$$

According to [17], the exergy factor for natural gas is equal to $1.04 \pm 0.5\%$.

The electricity provided by the gas turbine is 100% exergy, and the exergy rate of the output electricity is:

$$\dot{E}x_{GT}^{e}(t) = \dot{E}_{GT}(t) \tag{8}$$

The exergy rate of the output exhaust gas, $\dot{E}x_{GT}^{exgas}(t)$, is calculated by multiplying the energy rate by the related Carnot factor, since the temperature of the exhaust gas is assumed to be constant [1]:

$$\dot{E}x_{GT}^{exgas}(t) = \dot{Q}_{GT}^{exgas}(t)F_q(t) \tag{9}$$

with the Carnot factor, $F_q(t)$, expressed as:

$$F_q(t) = 1 - T_0(t)/T_{exgas}^{s} \tag{10}$$

which depends on the temperature of exhaust gas, T_{exgas}^{s}, and the reference temperature $T_0(t)$. By following the dynamic exergy analysis, hourly ambient temperatures are considered as reference temperatures [18].

The total exergy loss rate in the gas turbine is:

$$\dot{E}xloss_{GT}(t) = \dot{E}x_{GT}^{NG}(t) - \dot{E}_{GT}(t) - \dot{E}x_{GT}^{exgas}(t) \tag{11}$$

2.1.2. Meeting demand

The electricity rate demand, $\dot{E}_{dem}(t)$, and the electricity rate required by the heat pump, $\dot{E}_{HP}(t)$, must be covered by the sum of the electricity rate provided by the gas turbine, $\dot{E}_{GT}(t)$, and the electricity rate from the grid, $\dot{E}_{buy}(t)$:

$$\dot{E}_{dem}(t) + \dot{E}_{HP}(t) = \dot{E}_{GT}(t) + \dot{E}_{buy}(t) \tag{12}$$

In order to consider all the exergy losses at the energy conversion step, the exergy losses occurring in the power generation plants are also included. The exergy efficiency of power generation plants, ε_{gen}, is based on the technologies used in the plants, and the exergy loss rate is [19]:

$$\dot{E}xloss_{grid}(t) = \dot{E}_{buy}(t)/\varepsilon_{gen} - \dot{E}_{buy}(t) \tag{13}$$

2.2. Modeling of energy network for space heating

A typical energy network for space heating is shown in Fig. 2. The exhaust heat recovered in the heat recovery boiler is stored through the heat exchanger in a large water tank, which is used to supply hot water to buildings with a constant mass flow rate. A fully-mixed tank model is assumed for simplicity, where the water in the tank has a uniform time-varying temperature, because of the charge and discharge processes with a given efficiency. As to the water temperature in the tank, there are two cases. If the temperature is higher than the required (assumed constant), the water is directly supplied to the buildings and part of the water is mixed with the return water from buildings in the mixer. After mixing, the temperature of the mixed water is brought to the required one, and then the water is sent to the terminal devices in buildings. In the second case, if the temperature of the water tank is lower than the requirement, the water is sent to the auxiliary natural gas boiler or to the heat pump, and heated to the required temperature.

2.2.1. Modeling of the heat recovery boiler

Heat is recovered from the high-temperature exhaust gas in the heat recovery boiler. For simplicity, two heat recovery boilers are considered for space heating and domestic hot water, respectively. The modeling of more heat recovery boilers is similar, and the configuration of the energy network may become more complicated as the number of heat recovery boilers increases. The exhaust gas from the gas turbine is subdivided between the two heat recovery boilers. The sum of fractions of exhaust gas (continuous decision variable) for space heating, $\xi_{SH}(t)$, and domestic hot water, $\xi_{DHW}(t)$, has to be one:

$$\xi_{SH}(t) + \xi_{DHW}(t) = 1 \tag{14}$$

The heat rate delivered by the exhaust gas to the heat recovery boiler for space heating, $\dot{H}_{HRB,SH}(t)$, is:

Please cite this article in press as: Bing Yan, et al., Exergy-based operation optimization of a distributed energy system through the energy-supply chain, Applied Thermal Engineering (2016), doi: 10.1016/j.applthermaleng.2016.02.029

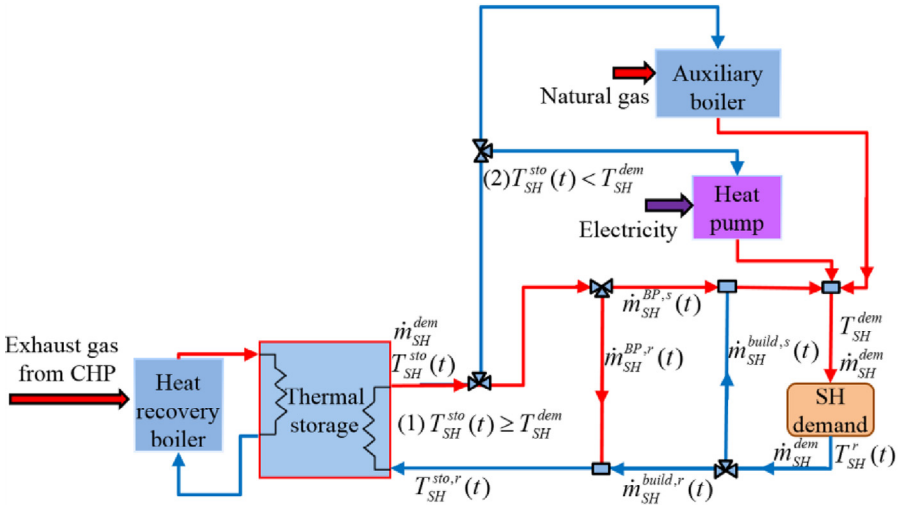

Fig. 2. Scheme of the energy network for space heating.

$$\dot{H}_{HRB,SH}(t) = \xi_{SH}(t)\eta_{HRB}\dot{Q}_{GT}^{exgas}(t) \tag{15}$$

where η_{HRB} is the heat recovery efficiency of the boiler. The heat balance equation is:

$$\begin{aligned}\dot{H}_{HRB,SH}(t) &= c_p\dot{m}_{HRB,SH}(t)\left(T_{HRB,SH}^{s} - T_{HRB,SH}^{r}(t)\right)\\ &= \eta_{hex}c_p\dot{m}_{HRB,SH}(t)\left(T_{HRB,SH}^{s} - T_{SH}^{sto}(t)\right)\end{aligned} \tag{16}$$

where c_p is the specific heat of water; $\dot{m}_{HRB,SH}(t)$ is the water mass flow rate through the heat exchanger in the storage from the heat recovery boiler (decision variable); $T_{HRB,SH}^{s}$ and $T_{HRB,SH}^{r}(t)$ are the temperatures of the water flowing into and out of the heat exchanger, respectively; $T_{SH}^{sto}(t)$ is the temperature of the water in the tank; and η_{hex} is the efficiency of the heat exchanger. The supply temperature and heat exchanger efficiency are assumed known, and the return temperature is a dependent variable.

The exergy input rate to the heat recovery boiler is its fraction of exhaust gas multiplied by the exergy rate of exhaust gas. At the output, the exergy rate of the heat delivered by the heat recovery boiler, $\dot{E}x_{HRB,SH}^{out}(t)$, is related to the mass flow rate and supply and return temperatures:

$$\dot{E}x_{HRB,SH}^{out}(t) = c_p\dot{m}_{HRB,SH}(t)\left[\left(T_{HRB,SH}^{s} - T_{HRB,SH}^{r}(t)\right) - T_0(t)\ln\left(\frac{T_{HRB,SH}^{s}}{T_{HRB,SH}^{r}(t)}\right)\right] \tag{17}$$

The exergy loss rate in the heat recovery boiler is:

$$\dot{E}xloss_{HRB,SH}(t) = \xi_{SH}(t)\dot{E}x_{GT}^{exgas}(t) - \dot{E}x_{HRB,SH}^{out}(t) \tag{18}$$

2.2.2. Modeling of the auxiliary natural gas boiler

The auxiliary natural gas boiler converts natural gas into heat for the space heating demand. The natural gas volumetric flow rate required by the boiler to provide the heat rate, $\dot{H}_{boil,SH}(t)$, is given by:

$$\dot{G}_{boil,SH}(t) = \dot{H}_{boil,SH}(t)/(\eta_{boil}LHV_{NG}) \tag{19}$$

where η_{boil} is the combustion efficiency of the boiler. The heat balance equation for the boiler is:

$$\dot{H}_{boil,SH}(t) = c_p\dot{m}_{SH}^{dem}\left(T_{boil,SH}^{s}(t) - T_{boil,SH}^{r}(t)\right) \tag{20}$$

where:

$$T_{boil,SH}^{s}(t) = T_{SH}^{dem} \text{ and } T_{boil,SH}^{r}(t) = T_{SH}^{sto}(t) \tag{21}$$

where $T_{boil,SH}^{s}(t)$ and $T_{boil,SH}^{r}(t)$ are the temperatures of the water flowing out and into of the boiler, respectively.

The input energy carrier to the boiler is natural gas. Similarly to the gas turbine, the exergy input rate of natural gas to the boiler, $\dot{E}x_{boil,SH}^{NG}(t)$, is the natural gas volumetric flow rate consumed by the boiler multiplied by the specific chemical exergy of natural gas, ex_{NG}. At the output, the exergy rate of the heat delivered by the boiler, $\dot{E}x_{boil,SH}^{out}(t)$, is evaluated similarly to that of the heat recovery boiler, based on the mass flow rate and supply and return temperatures. The exergy loss rate in the natural gas boiler is:

$$\dot{E}xloss_{boil,SH}(t) = \dot{E}x_{boil,SH}^{NG}(t) - \dot{E}x_{boil,SH}^{out}(t) \tag{22}$$

2.2.3. Modeling of the heat pump

The heat pump converts electricity into heat for the space heating demand. The electricity consumption, $\dot{E}_{HP}(t)$, of the heat pump to provide the heat rate, $\dot{H}_{HP}(t)$, is:

$$\dot{E}_{HP}(t) = \dot{H}_{HP}(t)/COP_{HP} \tag{23}$$

where COP_{HP} is the coefficient of performance. The heat balance equation for the heat pump is:

$$\dot{H}_{HP}(t) = c_p\dot{m}_{SH}^{dem}\left(T_{HP}^{s}(t) - T_{HP}^{r}(t)\right) \tag{24}$$

where:

$$T_{HP}^{s}(t) = T_{SH}^{dem} \text{ and } T_{HP}^{r}(t) = T_{SH}^{sto}(t) \tag{25}$$

where $T_{HP}^{s}(t)$ and $T_{HP}^{r}(t)$ are the temperatures of the water flowing out and into of the heat pump, respectively.

For the heat pump, electricity is the input energy carrier. The exergy input rate of electricity, $\dot{E}x_{HP}^{e}(t)$, is equal to the electricity consumption of the heat pump. At the output, the exergy rate of the heat delivered by the heat pump, $\dot{E}x_{HP}^{out}(t)$, is evaluated similarly to that of the heat recovery and auxiliary natural gas boilers. The exergy loss rate in the heat pump is:

$$\dot{E}xloss_{HP}(t) = \dot{E}x_{HP}^{e}(t) - \dot{E}x_{HP}^{out}(t) \tag{26}$$

Please cite this article in press as: Bing Yan, et al., Exergy-based operation optimization of a distributed energy system through the energy-supply chain, Applied Thermal Engineering (2016), doi: 10.1016/j.applthermaleng.2016.02.029

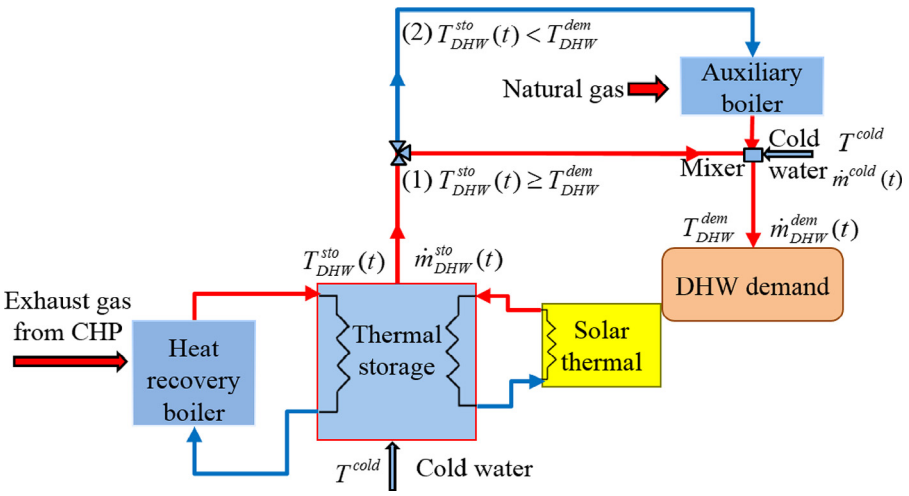

Fig. 3. Scheme of the energy network for domestic hot water.

2.2.4. Modeling of the thermal energy storage system

The energy stored in the water tank at time t is affected by: the energy stored at time $(t-\Delta t)$, the heat provided by the heat recovery boiler, and the heat supplied:

$$c_p m_{sto,SH} T^{sto}_{SH}(t) = \eta_{sto} c_p m_{sto,SH} T^{sto}_{SH}(t-\Delta t) + \left[\dot{H}_{HRB,SH} - c_p \dot{m}_{sto,SH}(t)\left(T^{sto}_{SH}(t) - T^{sto,r}_{SH}(t)\right)\right]\Delta t \quad (27)$$

where $m_{sto,SH}$ is the mass of water in the thermal storage and $T^{sto,r}_{SH}(t)$ is the temperature of the return water to the tank.

2.2.5. Meeting demand

The above devices are interconnected by the energy network through pipes. As mentioned earlier, there are two cases. In the first one, when the temperature of the water in the tank is higher than the required, T^{dem}_{SH}, the water is directly supplied to the buildings, and part of the water is mixed with the return water from buildings before going to the terminal devices inside the buildings:

$$\dot{m}^{dem}_{SH} = \dot{m}^{BP,s}_{SH}(t) + \dot{m}^{BP,r}_{SH}(t) = \dot{m}^{BP,s}_{SH}(t) + \dot{m}^{build,s}_{SH}(t) = \dot{m}^{build,s}_{SH}(t) + \dot{m}^{build,r}_{SH}(t) = \dot{m}^{BP,r}_{SH}(t) + \dot{m}^{build,r}_{SH}(t) \quad (28)$$

where $\dot{m}^{dem}_{SH}$ is the mass flow rate required to satisfy the space heating demand; $\dot{m}^{BP,s}_{SH}(t)$ is the bypass mass flow rate to be supplied to buildings; $\dot{m}^{BP,r}_{SH}(t)$ is the bypass mass flow rate to be returned to the tank; $\dot{m}^{build,s}_{SH}(t)$ is the return mass flow rate from buildings to be mixed with the water from the storage; and $\dot{m}^{build,r}_{SH}(t)$ is the return water mass flow rate from buildings to the tank. The energy balance in the mixer is expressed by:

$$c_p \dot{m}^{dem}_{SH} T^{dem}_{SH} = c_p \dot{m}^{BP,s}_{SH}(t) T^{sto}_{SH}(t) + c_p \dot{m}^{build,s}_{SH}(t) T^{r}_{SH}(t) \quad (29)$$

where $T^{r}_{SH}(t)$ is the temperature of the return water from buildings. After satisfying the space heating demand, the energy balance in the mixer is expressed by:

$$c_p \dot{m}^{dem}_{SH} T^{sto,r}_{SH}(t) = c_p \dot{m}^{BP,s}_{SH}(t) T^{sto}_{SH}(t) + c_p \dot{m}^{build,s}_{SH}(t) T^{r}_{SH}(t) \quad (30)$$

where $T^{sto,r}_{SH}(t)$ is the temperature of the return water to the water tank.

The heat balance equation at the demand side is:

$$\dot{H}^{dem}_{SH}(t) = c_p \dot{m}^{dem}_{SH}\left(T^{dem}_{SH} - T^{r}_{SH}(t)\right) \quad (31)$$

where $\dot{H}^{dem}_{SH}(t)$ is the heat rate demand of space heating.

In the second case, when the temperature of the water in the tank is lower than the required, the water is sent to the auxiliary natural gas boiler or the heat pump, and heated to the required temperature.

2.3. Modeling of energy network for domestic hot water

A typical energy network for domestic hot water is shown in Fig. 3. As in the previous subsection, a fully-mixed tank model is assumed. Since the water is used up at the demand side, cold water is continuously supplied to the storage and warmed up by the energy provided by the heat recovery boiler and solar collectors through two heat exchangers in the water tank.

There are two cases. When the temperature of the water in the tank is higher than the required (assumed constant), the water is directly supplied to the buildings and mixed with the aqueduct cold water in the mixer to bring down the temperature to the required one before the terminal use. In the second case, when the temperature of the water in the tank is lower than the required, the water is sent to the auxiliary natural gas boiler, and heated to the required temperature.

The energy and exergy modeling of the heat recovery boiler, auxiliary natural gas boiler, and thermal storage for domestic hot water is similar to the modeling of the corresponding devices for space heating.

2.3.1. Modeling of the solar thermal plant

The solar thermal plant converts solar energy into heat to meet the domestic hot water demand. The heat rate provided by the solar thermal plant, $\dot{H}_{ST}(t)$, is:

$$\dot{H}_{ST}(t) = \eta_{coll} A_{coll} \dot{I}_T(t) \quad (32)$$

where A_{coll} is the collector area, η_{coll} is the collector efficiency, and $\dot{I}_T$ is the total solar irradiance. The heat balance equation for the solar thermal plant is:

$$\dot{H}_{ST}(t) = c_p \dot{m}_{ST}(t)\left(T^{s}_{ST}(t) - T^{r}_{ST}(t)\right) = \eta_{hex} c_p \dot{m}_{ST}(t)\left(T^{s}_{ST}(t) - T^{sto}_{DHW}(t)\right) \quad (33)$$

where $\dot{m}_{ST}(t)$ is the water mass flow rate from the solar thermal plant through the heat exchanger in the storage; $T^{s}_{ST}(t)$ and $T^{r}_{ST}(t)$ are the temperatures of the water flowing into and out of the heat exchanger, respectively; and η_{hex} is the efficiency of the heat

Please cite this article in press as: Bing Yan, et al., Exergy-based operation optimization of a distributed energy system through the energy-supply chain, Applied Thermal Engineering (2016), doi: 10.1016/j.applthermaleng.2016.02.029

exchanger. The supply temperature is assumed 10 K higher than that of the water in the tank and the return temperature is a dependent variable.

Solar energy from the collectors is considered as a low-exergy source since the solar exergy input rate is evaluated at the output of the solar collector field [20]. Therefore, by following this approach no exergy loss is taken into account.

2.3.2. Meeting demand

Similarly to space heating, the above devices are interconnected by the energy network, and there are two cases. When the temperature of the water in the tank, $T^{sto}_{DHW}(t)$, is higher than the required, T^{dem}_{DHW}, the water is directly supplied to the buildings and mixed with the aqueduct cold water before the terminal use:

$$\dot{m}^{dem}_{DHW}(t) = \dot{m}^{sto}_{DHW}(t) + \dot{m}^{cold}(t) \tag{34}$$

where $\dot{m}^{dem}_{DHW}(t)$, $\dot{m}^{sto}_{DHW}(t)$, and $\dot{m}^{cold}(t)$ are the water mass flow rates to be supplied to terminal users, the hot water mass flow rate taken from the storage, and the cold water mass flow rate from the aqueduct, respectively. The energy balance in the mixer is expressed by:

$$c_p \dot{m}^{dem}_{DHW}(t) T^{dem}_{DHW} = c_p \dot{m}^{sto}_{DHW}(t) T^{sto}_{DHW}(t) + c_p \dot{m}^{cold}(t) T^{cold} \tag{35}$$

where T^{cold} is the temperature of the cold water from the aqueduct. At the demand side, it is assumed that the temperature of hot water is brought down to T^{cold} after terminal use, and the heat balance equation is:

$$\dot{H}^{dem}_{DHW}(t) = c_p \dot{m}^{dem}_{DHW}(t)\left(T^{dem}_{DHW} - T^{cold}\right) \tag{36}$$

where $\dot{H}^{dem}_{DHW}(t)$ is the heat rate demand of domestic hot water.

In the second case, when the temperature of the water in the tank, $T^{sto}_{DHW}(t)$, is lower than the required, T^{dem}_{DHW}, the water is sent to the auxiliary natural gas boiler:

$$\dot{m}^{dem}_{DHW}(t) = \dot{m}^{sto}_{DHW}(t) \tag{37}$$

The water is heated to the required temperature in the natural gas boiler.

For the overall problem, the coupling across the two energy networks is that the sum of exhaust fractions for space heating and domestic hot water has to be one (see Eq. (14)). The coupling across all the three networks is represented by the electricity balance (Eq. (12)).

2.4. Objective functions

The objective is to minimize the total energy cost and the exergy losses at the conversion step. The economic and exergetic objective functions are discussed in Subsections 2.4.1 and 2.4.2, respectively. The multi-objective optimization method to solve the problem is discussed in Subsection 2.4.3.

2.4.1. Economic objective

The economic objective is to minimize the total energy cost, *Cost*, which is the sum of two terms: cost of grid power and cost of natural gas:

$$Cost = \sum_t \Delta t\left(P_{grid}(t)\dot{E}_{buy}(t) + P_{gas}\dot{G}_{buy}(t)\right) \tag{38}$$

where $P_{grid}(t)$ is the time-of-day unit price of electricity from the power grid, and P_{gas} is the constant unit price of natural gas. The volumetric flow rate of natural gas bought, $\dot{G}_{buy}(t)$, corresponds to the total consumption requirement of the CHP system and auxiliary natural gas boilers.

2.4.2. Exergetic objective

As mentioned earlier, the focus of this paper is on the exergy loss at the energy conversion step, which accounts for the largest fraction of the total exergy losses in the energy-supply chain from energy resources to user demands. The total exergy loss at the conversion step, $Exloss_{conv}$, is the sum of the exergy losses of the energy devices at the conversion step over time:

$$\begin{aligned} Exloss_{conv} = \sum_t \Delta t\Big(&\dot{E}xloss_{GT}(t) + \dot{E}xloss_{grid}(t) \\ &+ \dot{E}xloss_{HRB,SH}(t) + \dot{E}xloss_{HRB,DHW}(t) + \dot{E}xloss_{boil,SH}(t) \\ &+ \dot{E}xloss_{boil,DHW}(t) + \dot{E}xloss_{HP}(t)\Big) \end{aligned} \tag{39}$$

2.4.3. Multi-objective optimization method

With the exergetic objective function formulated in Eq. (39) and the economic objective function formulated in Eq. (38), the problem has two objective functions to be minimized. To solve this multiple-objective problem, a single objective function is formulated as a weighted sum of the total energy cost, *Cost*, and the total exergy loss at the conversion step, $Exloss_{conv}$:

$$F_{obj} = c(1-\omega)Cost + \omega Exloss_{conv} \tag{40}$$

where the constant c is chosen such that c *Cost* and $Exloss_{conv}$ have the same order of magnitude. The Pareto frontier involving the best possible trade-offs between the two objectives can be found by varying the weight ω in between the interval 0 and 1. The solution that minimizes the total energy cost is obtained when $\omega = 0$, whereas the solution that minimizes the total exergy loss at the energy conversion step is obtained when $\omega = 1$. The above problem is separable, nonlinear and involves both discrete and continuous variables.

3. Solution methodology

To coordinate energy devices with coupling constraints and solve the problem efficiently, our idea is to use multipliers as shadow prices in a decomposition and coordination structure. Surrogate Lagrangian relaxation and branch-and-cut are combined for a speedy and near-optimal performance [21–23]. After relaxing the coupling constraints, i.e., CHP exhaust gas sharing constraints (Eq. (14)) by Lagrangian multipliers, the relaxed problem is to minimize the following Lagrangian function, L, as:

$$\begin{aligned} L(\lambda, y) \equiv\ & c(1-\omega)Cost(y) + \omega Exloss_{conv}(y) \\ &+ \sum_t \lambda(t)\left(\xi_{SH}(t) + \xi_{DHW}(t) - 1\right) \end{aligned} \tag{41}$$

subject to Eqs. (1)–(13) and (15)–(39). In the above, λ represent multipliers relaxing CHP exhaust gas sharing constraints, and y represent all the decision variables.

Then, there are two subproblems, e.g., the space heating subproblem and the domestic hot water subproblem (with electricity-related devices). They are solved by branch-and-cut individually.

By solving the relaxed problem, the dual function becomes:

$$q(\lambda) = \min_y L(\lambda, y) \tag{42}$$

Instead of obtaining the dual value in Eq. (42), a surrogate dual value is obtained in surrogate Lagrangian relaxation as follows:

$$\tilde{L}(\lambda^k, y^k) = c(1-\omega)Cost(y) + \omega Exloss_{conv}(y) + \lambda^k \tilde{g}(y^k) \tag{43}$$

Please cite this article in press as: Bing Yan, et al., Exergy-based operation optimization of a distributed energy system through the energy-supply chain, Applied Thermal Engineering (2016), doi: 10.1016/j.applthermaleng.2016.02.029

In the above, λ^k and y^k are multipliers and any feasible solution of the relaxed problem at iteration k, respectively, and $\tilde{g}(y^k)$ are the surrogate subgradient vectors consisting of:

$$\tilde{g}(y^k) = \xi_{SH}(t) + \xi_{DHW}(t) - 1 \tag{44}$$

Since surrogate Lagrangian relaxation does not require the relaxed problem to be fully optimized, surrogate subgradient directions may not form acute angles with directions toward optimal multipliers, which will cause divergence. To guarantee that surrogate directions form acute angles with directions toward the optimal multipliers, the relaxed problem has to be sufficiently optimized, such that surrogate dual values in Eq. (43) satisfy the surrogate optimality condition:

$$\tilde{L}(\lambda^k, y^k) < \tilde{L}(\lambda^k, y^{k-1}) \tag{45}$$

where y^{k-1} is a feasible solution at the iteration k^-1. Since the relaxed problem is not fully optimized and subgradient directions do not change much at each iteration, computational requirements and zigzagging of multipliers are much reduced as compared to traditional subgradient methods.

In the method, multipliers are updated as:

$$\lambda^{k+1} = \lambda^k + d^k \tilde{g}(y^k) \tag{46}$$

where d^k is the stepsize. It has been proven that the multipliers converge to the optimum if the stepsizes are updated by using the novel step-sizing formula developed in [21].

To solve subproblems by using branch-and-cut, which is suitable for mixed-integer linear problems, a linear formulation is needed [24,25]. Usually, the logarithm function can be linearly approximated within a small range. For other nonlinear terms such as cross product, the linearization is not easy. In the framework of surrogate Lagrangian relaxation, solutions from the previous iteration can be used as input data in the next iteration. Therefore the nonlinear terms can be linearly approximated by using the values of the previous solution under the monotonic condition as proved in [22]. The resulting linear problem will be optimized and the previous solution will be updated.

4. Numerical testing

The method discussed above has been implemented by using the commercial branch-and-cut solver IBM ILOG CPLEX Optimization Studio Version 12.6 on a PC with 2.90 GHz Intel (R) i7 CPU and 16 GB RAM. The targeted end-user is a large hypothetic hotel in Beijing with an area of 30,000 m^2. Worldwide, China is ranked third in energy consumption in commercial building sector [26], and the application of DESs has increased rapidly in recent years because of the supportive government policies and financial incentives [27]. A typical winter day of January is chosen, with one hour as time-step. The input data for the optimization model are first described in Subsection 4.1. Then, the Pareto frontier is presented and the operation strategies under different weights are discussed for different trade-off points in Subsection 4.2. The exergy losses of each step in the energy-supply chain obtained by the energy cost minimization and exergy loss minimization are also presented. In addition, the effects of energy resource prices are discussed. Finally, the comparison among different DES configurations is discussed in Subsection 4.3.

4.1. Input data

The hourly electricity, domestic hot water and space heating rate demands for a typical winter day of January are taken from a comprehensive investigation about energy demands of hotels in Beijing [28], and they are shown in Fig. 4. The time-of-day unit price of electricity from the power grid is also shown in Fig. 4 [29]. The exergy efficiency of the power generation plant is assumed equal to 0.32, a typical value when electricity is mostly generated by coal-fired thermal power plants as in China. The unit price of natural gas is assumed equal to 0.38 \$/Nm^3 [29], where Nm^3 stands for the volume of gas at 0 °C temperature and at 1.013 bar pressure. Its exergy factor is assumed equal to 1.04 [17].

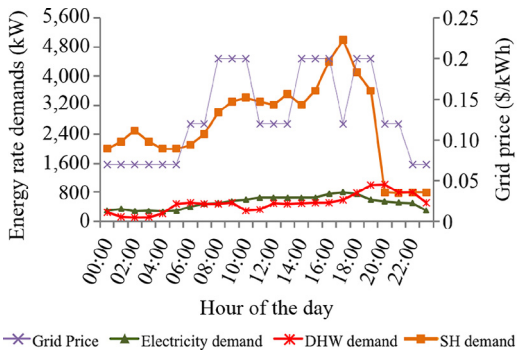

Fig. 4. Energy rate demands of the hotel and grid price for a typical winter day of January.

To evaluate the heat rate provided by the solar thermal plant, the hourly solar irradiance of a winter day is evaluated as the average of the solar irradiance of corresponding hours of all January days [30]. The sizes of the energy devices and thermal storages as well as the efficiencies assumed in this work are listed in Table 1.

4.2. Pareto frontier

Based on the network configurations shown in Figs. 2 and 3, there are non-linearizable logic constraints. The Surrogate Lagrangian relaxation method combined with branch-and-cut is suitable for mixed-integer linear problems. To get a linear problem and test this innovative optimization method, temperatures of the water in the tanks are hypothesized lower than the required temperatures in the numerical testing. This assumption is supported by the fact that, in winter days, solar radiation is in general lower than in summer days, and electricity demand is also lower. As a consequence, water temperature in the storage tanks can be lower than that required for most of the day.

The optimization problem can be solved within several minutes and the Pareto frontier is shown in Fig. 5. The point marked with *a* is obtained by minimizing the total energy cost, and the daily energy cost is 3487 \$/d whereas the daily exergy losses at the conversion step are 75,459 kJ/d. The point marked with *b* is obtained by minimizing the total exergy losses at the conversion step. The

Table 1
Size and efficiency of energy devices and thermal storages.

Primary energy devices	Size (MW)	Efficiency	
		Electrical	Thermal
Gas turbine	1.25	0.24	$\mu_{GT} = 0.080$
Solar thermal plant	0.41		0.40
Secondary energy devices	Size (MW)	Efficiency	
Heat pump	5.0	$COP_{SH}^{HP} = 3.0$	
Heat recovery boiler SH – DHW	2.4–1.1	$\eta_{HRB} = 0.80$	$\eta_{boiler} = 0.90$
Thermal energy storage	Capacity (MWh)	Efficiency	
SH – DHW	0.064–0.24	0.98	

Please cite this article in press as: Bing Yan, et al., Exergy-based operation optimization of a distributed energy system through the energy-supply chain, Applied Thermal Engineering (2016), doi: 10.1016/j.applthermaleng.2016.02.029

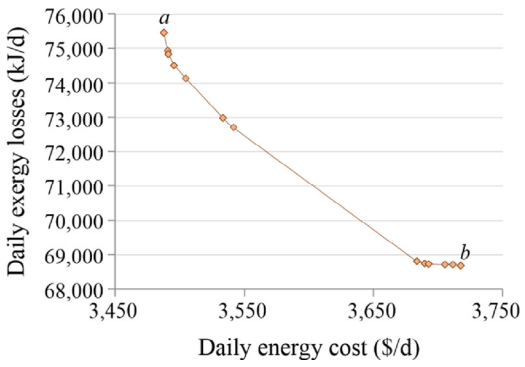

Fig. 5. Pareto frontier.

daily energy cost is 3718 $/d whereas the daily exergy losses are 68,687 kJ/d. The points between the extreme points are found by subdividing the weight interval into 100 equally-spaced points. There are 13 points since some solutions have been found under more than one weight values.

Each point on the Pareto frontier corresponds to a different operation strategy of the DES. In order to understand how the operation strategies vary with the weight ω, the optimized operation strategies of the DES obtained by varying the weight from 0 to 1 with a 0.1 increase, are presented in Fig. 6.

Fig. 6a shows that, when ω varies from 0 to 1 (from energy cost minimization to exergy loss minimization), the share of the electricity load (sum of electricity demand and electricity required by the heat pump) satisfied by the CHP system increases while the exergy losses reduce. This highlights the essential role of the CHP system in the reduction of exergy losses because of the recovery of waste heat for thermal purposes, leading to efficient use of the high-quality energy resource.

Fig. 6b shows that from energy cost minimization to exergy loss minimization, the share of space heating demand satisfied by the heat recovery boiler increases, coherent with the increasing use of the CHP (as shown in Fig. 6a), highlighting the importance of waste heat recovery for the exergetic purpose. The use of exhaust gas for low-exergy thermal demands reduces the exergy losses occurring at the energy conversion step. When ω varies from 0 to 1, the share of space heating demand met by the heat pump exhibits an opposite trend, decreasing with the reduced use of the grid power, as shown in Fig. 6a.

Fig. 6c shows that from energy cost minimization to exergy loss minimization, the share of the domestic hot water demand satisfied by the heat recovery boiler increases coherently with the increased use of the CHP system. Conversely, the share of domestic hot water demand satisfied by the auxiliary natural gas boiler reduces, highlighting that natural gas as a high-quality energy resource should not be used for low-quality thermal demands, thereby reducing the waste of high-quality energy resources.

Fig. 7 shows the exergy losses occurring at the various steps of the energy-supply chain (i.e., conversion, storage, terminal devices, final consumption) under cost and exergy loss (at the conversion step) minimization. Exergy losses occurring in the storages and in the terminal devices as well as exergy of user demands are evaluated according to Reference [1]. In the exergy loss minimization, exergy losses at the conversion step are about 9% lower than those obtained by energy cost minimization. On the other hand, exergy losses occurring in the storages are 22% higher than those obtained under energy cost minimization. This is because, under exergy loss minimization, there is larger use of heat recovery boilers, which charge the storages, than what occurs under energy cost minimization, as shown in Fig. 6B and C. This means that the minimization

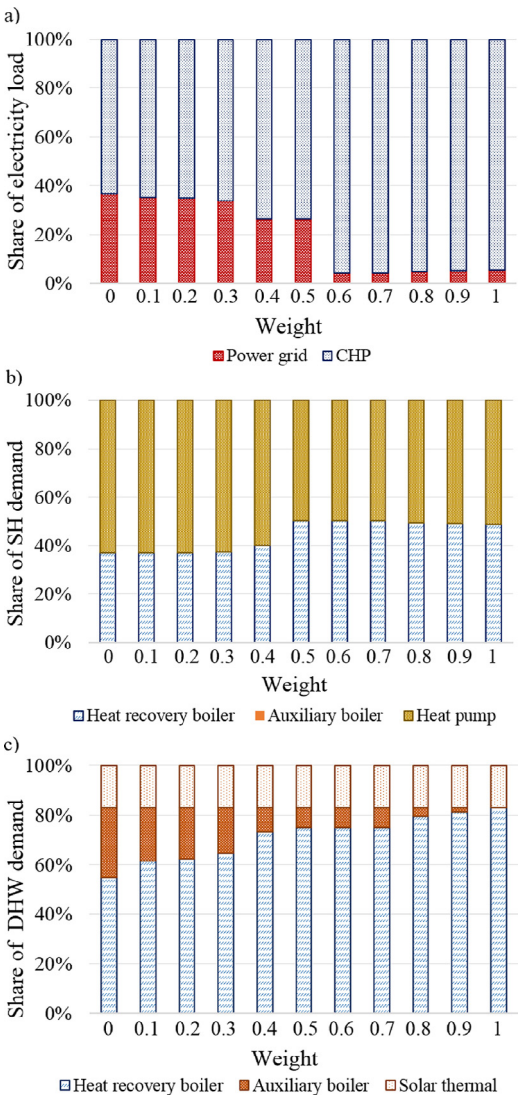

Fig. 6. Optimized operation strategies of the DES at various trade-off points for a) electricity, b) space heating, c) domestic hot water.

of exergy losses at the conversion step does not guarantee the minimization of exergy losses in the other steps of the energy-supply chain. However, the total exergy loss occurring in the whole energy-supply chain under exergy loss minimization is 7% lower than that obtained under cost minimization.

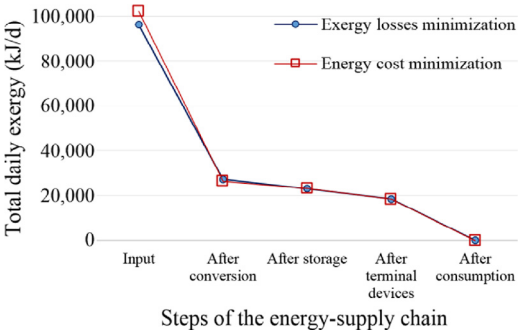

Fig. 7. Exergy losses of each step in the energy-supply chain under cost and exergy losses minimization.

Please cite this article in press as: Bing Yan, et al., Exergy-based operation optimization of a distributed energy system through the energy-supply chain, Applied Thermal Engineering (2016), doi: 10.1016/j.applthermaleng.2016.02.029

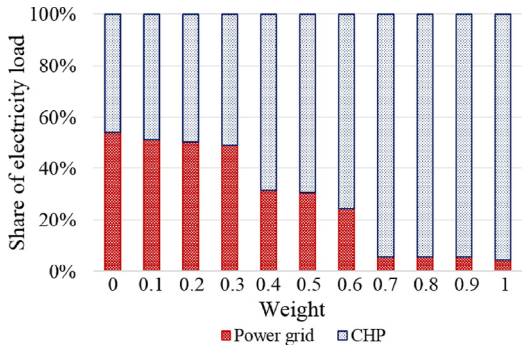

Fig. 8. Optimized operation strategies of the DES at various trade-off points for electricity with a high natural gas price.

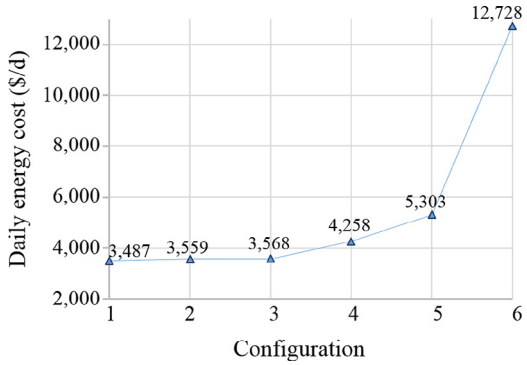

Fig. 9. Total daily energy costs under energy cost minimization for Configurations 1–6.

The optimized operation strategies of the DES depend on the prices of energy resources. In the problem under consideration (reference case), the price of natural gas is cheaper than that of grid power as in the current Chinese market. To show how the relative prices of natural gas and grid power affect the optimized operation strategies, the problem is solved with a natural gas price as 150% of the price considered in the reference case.

Fig. 8 shows the optimized operation strategies for electricity at the various trade-off points with a high natural gas price. It is shown that the share of the electricity load satisfied by the CHP system increases from energy cost minimization to exergy loss minimization, as occurs in the reference case, as shown in Fig. 6a. However, compared to the reference case, the share of electricity load covered by the CHP system is generally lower when the weight of the economic objective is higher than that of the exergetic one, and almost the same when the weight of the economic objective is lower. In particular, when $\omega = 0$, 0.3 and 0.5, the share of the electricity load covered by the CHP system is 46%, 51% and 69% in the new case, respectively, whereas it is 63%, 66% and 74% in the reference case, respectively. The lower usage of the CHP system results in lower amount of exhaust gas and consequent higher usage of auxiliary boilers for thermal purposes. This leads to higher exergy losses at the energy conversion step as compared to the reference case.

4.3. Configuration comparison

To show how each energy device contributes to the reduction of energy costs and exergy losses, various configurations of the DES are now analyzed. For each configuration, one energy device is taken out of the DES, including the solar thermal plant, auxiliary natural gas boilers, heat pump, and entire CHP system. In addition, a conventional energy supply system is also considered. The grid power is used to meet the electricity demand, the electricity required by an electric heater to satisfy the space heating demand, and the electricity required by an electric boiler to satisfy the domestic hot water demand. All the above configurations are listed in Table 2.

Table 2
Investigated configurations.

Configuration	Energy devices taken out of the reference case (Configuration I)
1	With all devices
2	Without solar thermal plant
3	Without auxiliary natural gas boilers
4	Without heat pump
5	Without CHP system
Configuration	Conventional energy supply system
6	All from grid power

The daily energy costs obtained under cost minimization of different configurations are compared in Fig. 9. Configuration 1 is the reference case, consisting of all energy devices listed in Table 1. The reference case shows the best performance in terms of the daily energy costs as compared with the other configurations. For Configurations 2 and 3, the daily energy costs are about 2% larger than those in Configuration 1. For Configuration 4, the daily energy costs are 18% higher than those in Configuration 1, because of the high conversion efficiency of the heat pump. Configuration 5 excludes the CHP system. The costs are 34% larger than those in Configuration 1, pointing out the essential role of the CHP system in the reduction of energy costs. The worst case is represented by the conventional energy supply system (Configuration 6). The 73% increase in the daily energy costs, as compared with Configuration 1, shows that the energy costs can be strongly reduced by the optimized operation of the DES.

Fig. 10 shows the exergy losses occurring at different steps of the energy-supply chain obtained by the exergy loss (at the conversion step) minimization for the configurations listed in Table 2. The reference case (Configuration 1) shows the best performance, also in terms of minimum exergy losses at the conversion step. For Configuration 2, exergy losses increase by 2% as compared with Configuration 1. For Configuration 3, the exergy losses are the same as those in Configuration 1, since in the exergy loss minimization the auxiliary boilers are never used to satisfy the domestic hot water and space heating demands, as shown in Fig. 6b and c. The exergy losses for Configuration 4 (without the heat pump), are 22% larger than those in Configuration 1, showing the importance of the heat pump not only in the reduction of energy costs but also in the reduction of exergy losses, thanks to its high conversion efficiency. A 28% increase in

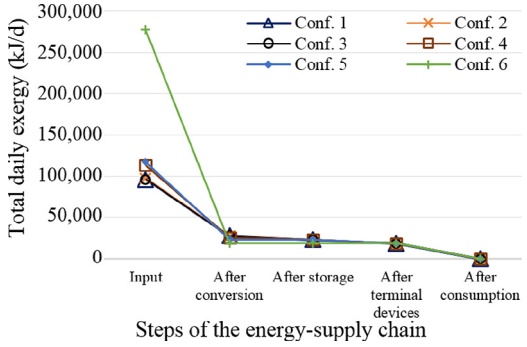

Fig. 10. Exergy losses of each step in the energy-supply chain under exergy loss minimization for Configurations 1–6.

Please cite this article in press as: Bing Yan, et al., Exergy-based operation optimization of a distributed energy system through the energy-supply chain, Applied Thermal Engineering (2016), doi: 10.1016/j.applthermaleng.2016.02.029

the exergy losses is found for Configuration 5, as compared with Configuration 1. Without the CHP system, there is no exhaust gas for heat, and the use of auxiliary boilers increases the exergy losses because of the combustion processes. Finally, similarly to the energy costs, the worst case is represented by Configuration 6, where the exergy losses are 73% larger than those in Configuration 1. When all the demands are satisfied by electricity, high exergy losses occur, since a high quality energy carrier, electricity, is used to satisfy low-quality thermal demands.

Exergy losses in thermal storages do not reach the minimum value in the reference case. The minimum value is obtained in Configuration 5, which is 93% lower than that in the reference case. Without the CHP system, the SH storage is not used with consequent zero exergy losses, and the DHW storage is only charged by the solar thermal collectors. Therefore, the total exergy loss is reduced at the storage step. However, the total exergy loss occurring in the whole energy-supply chain reaches the minimum in the reference case as compared with other configurations.

5. Conclusions

This paper analyzes the exergy-efficient management of the energy-supply chain of a DES to reduce both energy costs and exergy losses at the conversion step. A mixed-integer optimization problem considering several energy devices is formulated and is solved by surrogate Lagrangian relaxation combined with branch-and-cut. The objective is to minimize a weighted sum of energy costs and exergy losses at the conversion step. Numerical results show that when both fossil and renewable energy resources are appropriately combined under the optimized operation of the DES, energy costs and exergy losses can be reduced. The use of high-quality energy resources can be reduced through the reduction of exergy losses at the energy conversion step, which are the largest part in the whole energy-supply chain, leading to sustainability of energy supply systems. The operators of DESs can choose the operation strategy from the Pareto frontier based on cost and sustainability concerns. Future work may include exergy-efficient management of the various steps of the energy supply chain, from energy resources to user demands, to reduce the total exergy loss of each sub-process.

Acknowledgment

Authors thank the Università degli Studi di Napoli Federico II for funding this study within the agreement with the University of Connecticut and the Smart grid con sistemi di poligenerazione distribuita (Poligrid) project.

Nomenclature

A	Area (m^2)
c	Constant in Eq. (40) (kWh/$)
c_p	Specific heat of water (kJ/kg/K)
COP	Coefficient of performance
$Cost$	Total energy cost ($)
d	Stepsize in Eq. (46)
DR	Maximum ramp-down rate (kW)
ex_{NG}	Specific chemical exergy of natural gas (kWh/Nm^3)
$\dot{E}$	Electricity rate (kW)
$\dot{E}x$	Exergy rate (kW)
$\dot{E}xloss$	Exergy loss rate (kW)
$Exloss_{conv}$	Total exergy loss at energy conversion step (kJ)
F_{obj}	Objective function
F_q	Carnot factor
$\tilde{g}$	Surrogate subgradient vectors
$\dot{G}$	Natural gas volumetric flow rate (Nm^3/h)
$\dot{H}$	Heating rate (kW)
$\dot{I}_T$	Total solar irradiance (kW/m^2)
L	Lagrangian function
$\tilde{L}$	Surrogate dual value
LHV_{NG}	Natural gas lower heat value (kWh/Nm^3)
$\dot{m}$	Mass flow rate (kg/h)
m	Mass (kg)
P_{gas}	Natural gas price ($/$Nm^3$)
P_{grid}	Electricity price ($/kWh)
q	Dual function
$\dot{Q}_{GT}^{exgas}$	Heat rate made available by the exhaust gas (kW)
R	Energy generation rate (kW)
S	Energy source input rate (kW)
t	Time (h)
T	Temperature (K)
UR	Maximum ramp-up rate (kW)
x	Binary decision variable
y	All the decision variables in Eq. (41)

Greek symbols

Δt	Length of the time interval (h)
ε_{gen}	Exergy efficiency of electricity generation
ς	Exergy factor
η	Efficiency
λ	Lagrangian multipliers
μ_{GT}	Percent heat loss rate of the gas turbine
ξ	Gas turbine exhaust fraction
ω	Weight in Eq. (40)

Superscript/Subscripts

0	Reference
boil	Boiler
BP	Bypass
build	Building
buy	Bought
cold	Cold
coll	Collector
dem	Demand
DHW	Domestic hot water
e	Electricity
ED	Energy device
exgas	Exhaust gas
NG	Natural gas
grid	Power grid
GT	Gas turbine
hex	Heat exchanger
HP	Heat pump
HRB	Heat recovery boiler
in	Input
k	Iteration
max	Maximum
min	Minimum
out	Output
r	Return
s	Supply
SH	Space heating
ST	Solar thermal
sto	Thermal storage

Acronyms

CHP	Combined heat and power
DES	Distributed energy system
DHW	Domestic hot water
SH	Space heating

Please cite this article in press as: Bing Yan, et al., Exergy-based operation optimization of a distributed energy system through the energy-supply chain, Applied Thermal Engineering (2016), doi: 10.1016/j.applthermaleng.2016.02.029

References

[1] ECBCS, Annex 49 – low exergy systems for high performance buildings and communities, homepage. <http://www.ecbcs.org/annexes/annex49.htm> (accessed 30.03.15).
[2] Eurostat Statistics Database, Energy statistics – supply, transformation, consumption, 2010.
[3] D. Schmidt, Low exergy systems for high performance buildings and communities, Energy Build. 41 (2009) 331–336.
[4] J. Szargut, International progress in second law analysis, Energy 5 (1980) 709–718.
[5] IEA/ECBCS Annex 37, Low exergy systems for heating and cooling, 2003.
[6] D. Schmidt, Design of low exergy buildings – method and a pre-design tool, Int. J. Low Energy Sustain. Build. 3 (2004) 1–2.
[7] J. Szargut, D.R. Morris, F.R. Stewerd, Exergy Analysis of Thermal, Chemical and Metallurgical Processes, Hemisphere, New York, 1988.
[8] A. Yildiz, A. Güngör, Energy and exergy analyses of space heating in buildings, Appl. Energy 86 (2009) 1939–1948.
[9] S.C. Jansen, J. Terès-Zubiaga, P.G. Luscuere, The exergy approach for evaluating and developing an energy system for a social dwelling, Energy Build. 55 (2012) 693–703.
[10] J. Terès-Zubiaga, S.C. Jansen, P. Luscuere, Dynamic exergy analysis of energy systems for a social dwelling and exergy based system improvement, Energy Build. 64 (2013) 359–371.
[11] A. Kari, S. Arto, Distributed energy generation and sustainable development, Renew. Sustain. Energy Rev. 10 (2006) 539–558.
[12] B. Yan, P.B. Luh, B. Sun, C. Song, C. Dong, Z. Gan, et al., Energy-efficient management of eco-communities, in: Proceedings of IEEE CASE, Madison, USA, 2013. Aug 17–20.
[13] X. Guan, Z. Xu, Q. Jia, Energy-efficient buildings facilitated by microgrid, IEEE Trans. Smart Grid 1 (2011) 466–473.
[14] G. Graditi, M. Ippolito, R. Lamedica, A. Piccolo, A. Ruvio, E. Santini, et al., Innovative control logics for a rational utilization of electric loads and air-conditioning systems in a residential building, Energy Build. 102 (2015) 1–17.
[15] M. Di Somma, B. Yan, N. Bianco, G. Graditi, P.B. Luh, L. Mongibello, et al., Operation optimization of a distributed energy system considering energy costs and exergy efficiency, Energy Convers. Manag. 103 (2015) 739–751.
[16] X.Q. Kong, R.Z. Wang, X.H. Huang, Energy optimization for a CCHP system with available gas turbines, Appl. Therm. Eng. 25 (2005) 377–391.
[17] K.J. Kotas, The Exergy Method for Thermal Plant Analysis, Reprinted, Krieger, Malabar, FL, 1995.
[18] A. Angelotti, P. Caputo, The exergy approach for the evaluation of heating and cooling technologies, first results comparing steady state and dynamic simulations, in: Proceedings of the 2nd PALENC and 28th AIVC Conference, vol. I, Crete Island, Greece, 2007, pp. 59–64. September 27–29.
[19] L.M. Ramirez-Elizondo, G.C. Paap, R. Ammerlaan, R.R. Negenborn, R. Toonssen, On the energy, exergy and cost optimization of multi-energy-carrier power systems, Int. J. Exergy 13 (2013) 364–385.
[20] H. Torìo, A. Angelotti, D. Schmidt, Exergy analysis of renewable energy-based climatisation systems for buildings: a critical view, Energy Build. 41 (2009) 248–271, M.A.
[21] M.A. Bragin, P.B. Luh, J.H. Yan, N. Yu, G.A. Stern, Convergence of the Surrogate Lagrangian Relaxation Method, J. Optim. Theory Appl. 164 (1) (2015) 173–201.
[22] M.A. Bragin, P.B. Luh, J.H. Yan, G.A. Stern, An efficient approach for solving mixed-integer programming problems under the monotonic condition, J. Control Decis. (2016) doi:10.1080/23307706.2015.1129916.
[23] M.A. Bragin, P.B. Luh, J.H. Yan, G.A. Stern, Novel exploitation of convex hull invariance for solving unit commitment by using surrogate Lagrangian relaxation and branch-and-cut, in: Proceedings of the IEEE Power and Energy Society, General Meeting. Denver, Colorado, 2015.
[24] R.E. Bixby, M. Fenelon, Z. Gu, E. Rothberg, R. Wunderling, MIP: theory and practice – closing the gap, Syst. Model. Optim. (2000) 19–49.
[25] IBM ILOG, "IBM ILOG CPLEX optimization studio information center," [Online]. <http://pic.dhe.ibm.com/infocenter/cosinfoc/v12r5/index.jsp> (accessed 10.01.15).
[26] Pacific Northwest National Laboratory, China's building energy use: a long-term perspective based on a detailed assessment. <http://www.pnnl.gov/main/publications/external/technical_reports/PNNL-21073.pdf>, January 2012 (accessed 15.01.16).
[27] J. Han, L. Ouyang, Y. Xu, R. Zeng, S. Kang, G. Zhang, Current status of distributed energy system in China, Renew. Sustain. Energy Rev. 55 (2016) 288–297.
[28] Z. Zhou, P. Liu, Z. Li, W. Ni, An engineering approach to the optimal design of distributed energy systems in China, Appl. Therm. Eng. 53 (2013) 387–396.
[29] Beijing Municipal Commission of Development & Reform, Current prices for public commodities. <http://www.bjpc.gov.cn/English/201512/t9802512.htm> (accessed 20.12.11).
[30] ASHRAE International Weather files for Energy Calculations (IWEC weather files), Users Manual and CD-ROM, American Society of Heating, Refrigerating and Air-Conditioning Engineers, Atlanta, GA, USA, 2001.

Please cite this article in press as: Bing Yan, et al., Exergy-based operation optimization of a distributed energy system through the energy-supply chain, Applied Thermal Engineering (2016), doi: 10.1016/j.applthermaleng.2016.02.029